TECHNICAL NOTE

Spin-Echo Echo-Planar Perfusion MR Imaging in the Differential Diagnosis of Solitary Enhancing Brain Lesions: Distinguishing Solitary Metastases from Primary Glioma

G.S. Young
K. Setayesh

SUMMARY: Unlike the more widely reported gradient-echo echo-planar perfusion-weighted imaging (EPI-PWI) technique, spin-echo (SE) EPI relative cerebral blood volume maps select for blood volume in microvessels <8 μm in diameter. This first report of SE-EPI PWI for distinguishing brain metastasis from high-grade glioma demonstrated 88% sensitivity and 72% specificity in 83 patients. We discuss differences in microvessel architecture between high-grade glioma and brain metastasis that may explain the surprising success of SE-EPI in this application and may deserve further investigation.

Distinction of brain metastasis from high-grade glioma by MR imaging remains an important unsolved clinical problem. Percentage recovery analysis of time-intensity curves from gradient-echo echo-planar (GE-EPI) dynamic susceptibility contrast perfusion-weighted imaging (PWI)[1] has been proposed to distinguish these tumor types by assessing increased capillary permeability in brain metastasis, but to our knowledge, no published report yet documents the accuracy of this method. Reports from the pathology literature suggest that in addition to permeability, brain metastasis and high-grade glioma neovessels differ substantially in vascular architecture,[2-7] and in particular, metastases may contain a substantially larger proportion of intermediate-sized dysplastic vessels up to 70 μm in diameter.[8-12] Recent literature demonstrates that spin-echo EPI (SE-EPI) PWI has a substantially different vessel-size sensitivity profile from GE-EPI PWI.[13-15] Because SE-EPI PWI relative cerebral blood volume (rCBV) maps reflect nearly exclusively the blood volume of microvessels <8 μm in diameter, in contrast to the admixture of microvessels and larger vessels assessed with GE-EPI, we hypothesized that SE-EPI rCBV maps would allow reliable distinction of brain metastasis from high-grade glioma. To our knowledge, this is the first report using SE-EPI PWI to make this distinction.

Technique

Forty-three subjects with high-grade glioma (20 cases of glioblastoma multiforme, 14 anaplastic astrocytomas, 7 anaplastic oligoastrocytomas, and 2 unspecified high-grade gliomas) and 40 patients with brain metastasis (2 sarcomas; 38 carcinomas, including 20 lung, 5 melanoma, 1 basal cell, 4 breast, 1 esophageal, 2 colorectal, 1 prostate; and 4 adenocarcinomas of unknown primary) were included chronologically from our institutional data base. Ninety-eight percent (42) of patients with high-grade glioma and 68% (27) of patients with brain metastasis had received previous chemotherapy; 63% (27) of patients with high-grade glioma and 85% of patients with metastasis (34) had received radiation (Table 1). Following institutional protocol, SE-EPI PWI (TE = 80 ms, TR = 1900–2216.7 ms, section thickness = 10 mm, matrix = 128^2–256^2) was performed by using a 4-mL/s bolus injection of 30-mL double-dose gadopentetate dimeglumine (Magnevist; Bayer HealthCare Pharmaceuticals, Wayne, NJ) (0.15–0.3 mmol/kg depending on body weight) and was coregistered with delayed postgadolinium T1-weighted imaging. Imaging was performed on 1.5T or 3T commercial MR imaging scanners (GE Healthcare, Milwaukee, Wis), and PWI data were processed by using a perfusion-processing software package (GADW 4.3 FuncTool software, GE Healthcare), which creates color rCBV maps by calculating the change in transverse relaxivity (R2) from signal-intensity measurements, integrates the area under the relaxivity curve and corrects for TE, according to the following standard formula:

$$rCBV = \sum_{i=0}^{N} \Delta R2_t = \frac{-1}{TE} \sum_{i=0}^{N} \ln\left(\frac{S_i}{S_0}\right).$$

Following previously published "hot spot" methods, we selected a roughly 100-mm^2 region of interest (ROI) within the region of maximal rCBV and recorded the average rCBV within the ROI as the rCBVmax.[16,17] We calculated a normalized rCBV (nCBV) by dividing rCBVmax by the rCBV of an equivalent ROI in the contralateral normal-appearing white matter[16] and performed percentage recovery analysis in the same ROI according to previously reported GE-EPI techniques.[1]

Results

The average nCBV within enhancing high-grade glioma was 1.53 ± 0.79 (0.59–4.05) compared with 0.82 ± 0.40 for brain metastasis (0.48–2.12), and differences between nCBV averages and ranges for the 2 groups were significant ($P < .05$) (Fig 1*C*). Sensitivity and specificity for detection of brain metastasis were 95% and 51%, respectively, by using an nCBV threshold of 1.3; and 36% and 93%, by using a 0.7 threshold. The optimal threshold occurred at 1.0, where sensitivity and specificity were 88% and 72% (Table 2).

Percentage recovery analysis yielded average signal-intensity recoveries of 0.86 for high-grade glioma and 0.75 for brain metastasis ($P < .05$). Percentage recovery analysis sensitivity and specificity to distinguish brain metastasis from high-grade glioma were 18% and 93% by using a previously reported[1] signal-intensity recovery threshold of 0.66. Optimal accuracy,

Received April 10, 2008; accepted after revision June 5.

From the Department of Radiology of Brigham and Women's Hospital, Harvard Medical School, Boston, Mass.

Both authors contributed equally to this work.

Please address correspondence to Geoffrey S. Young, MD, Brigham and Women's Hospital, Radiology Department, 75 Francis St, Boston, MA 02115; e-mail: GSYOUNG@PARTNERS.ORG

DOI 10.3174/ajnr.A1239

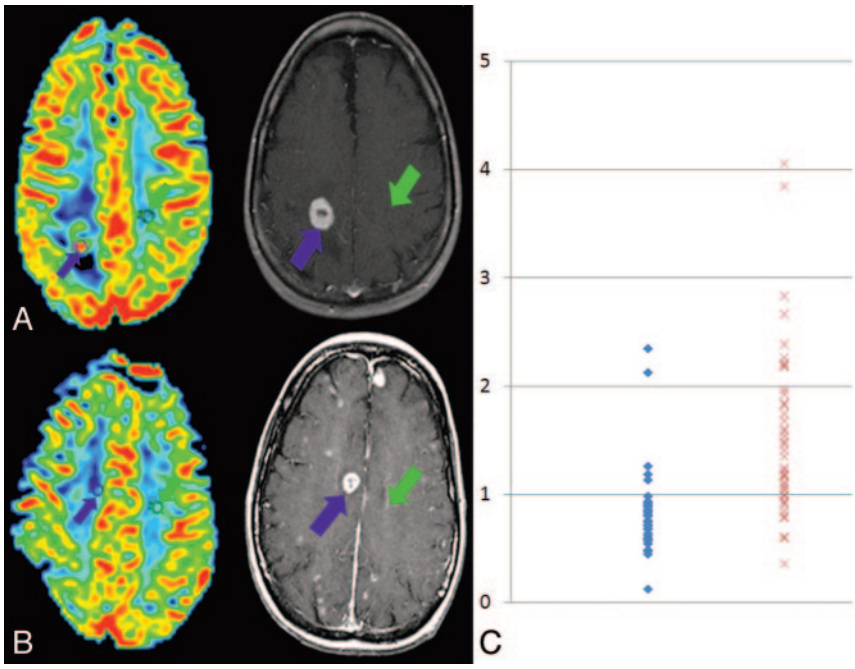

Fig 1. *A* and *B*, rCBV maps (*left*) demonstrate increased blood volume in the enhancing high-grade glioma (*A*) and decreased blood volume in the enhancing brain metastasis (*B*). Corresponding T1-weighted images are shown (*center*) with *black arrows* representing the location of ROI selection in the lesion and *white arrows* indicating control ROI location in normal appearing contralateral white matter placement. *C*, Scatterplot of the nCBV measurements in brain metastasis (*blue diamonds*) and high-grade glioma (*red squares*). (Color figure is available on-line only at www.ajnr.org.)

Table 1: Patient Demographics

	Age	Sex	Previous Chemotherapy	Previous Radiotherapy
Glioma	49.9 ± 11.21	21 F/22 M	98% (20 F/22 M)	63% (6 F/10 M)
Metastases	56.5 ± 11.60	18 F/22 M	68% (6 F/7 M)	85% (2 F/4 M)
Overall	53.1 ± 11.80	39 F/44 M	83% (7 F/7 M)	73% (8 F/14 M)

Note:—F indicates female; M, male.

Table 2: Diagnostic Accuracy of SE-EPI nCBV vs. Percent Recovery Using Optimal Thresholds of nCBV = 1.0 and % recovery = 66%

	nCBV	Percentage Recovery
Glioma	1.52 ± 0.78	0.85 ± 0.25
Metastases	0.82 ± 0.39	0.75 ± 0.15
Sensitivity	0.87	0.18
Specificity	0.72	0.93

Note:—nCBV indicates normalized cerebral blood volume.

obtained by using a signal-intensity recovery threshold of 0.85, yielded a sensitivity and specificity of 84% and 48% (Table 2).

Discussion

In this retrospective series, SE-EPI-derived rCBV maps allowed reliable distinction of brain metastasis from high-grade glioma and were superior to percentage recovery analysis for distinguishing brain metastasis from high-grade glioma by using SE-EPI (Fig 1). Because of the limitations regarding the retrospective design of this initial report, further study is required before this finding can be applied clinically. Most important, although both groups received radiation and chemotherapy, differences in treatment response between the groups could conceivably contribute to the differences observed.

Although definitive testing of our hypothesis that the success of SE-EPI is related to differences in vessel-size distribution between brain metastasis and high-grade glioma is beyond the scope of this report, a number of limitations of the current data deserve consideration in the design of future studies. First, as our percentage recovery analysis demonstrates, there is a significant difference between the brain metastasis and high-grade glioma groups in microvessel permeability. Future studies designed to investigate whether the observed effect is actually related to vessel-size differences between brain metastasis and high-grade glioma will require more rigorous correction for T1 shortening effects due to first-pass capillary leak.[18] Additionally, the use of interleaved GE-SE vessel-size imaging[5,6] may be of interest. Finally, because of the paucity of direct analyses of metastatic vessel-size distribution in the pathology literature, correlation with microscopic imaging would be valuable.

Conclusion

SE-EPI-derived rCBV maps promise to assist in accurate preoperative distinction of brain metastasis from high-grade glioma. If more rigorous analysis in treatment-naïve patients and prospective investigation support the preliminary findings presented here, SE-EPI PWI may prove an important clinical tool.

References

1. Cha S, Johnson G, Wadghiri YZ, et al. **Dynamic, contrast-enhanced perfusion MRI in mouse gliomas: correlation with histopathology.** *Magn Reson Med* 2003;49:848–55
2. Deane BR, Lantos PL. **The vasculature of experimental brain tumors. Part 1. A sequential light and electron microscope study of angiogenesis** *J Neurol Sci* 1981;49:55–66
3. Dennie J, Mandeville JB, Boxerman JL, et al. **NMR imaging of changes in vascular morphology due to tumor angiogenesis.** *Magn Reson Med* 1998;40:793–99

4. Kremer S, Grand S, Berger F, et al. **Dynamic contrast-enhanced MRI: differentiating melanoma and renal carcinoma metastases from high-grade astrocytomas and other metastases.** *Neuroradiology* 2003;45:44–49
5. Kiselev VG, Strecker R, Ziyeh S, et al. **Vessel size imaging in humans.** *Magn Reson Med* 2005;53:553–63
6. Tropres I, Grimault S, Vaeth A, et al. **Vessel size imaging.** *Magn Reson Med* 2001;45:397–408
7. Aronen HJ, Gazit IE, Louis DN, et al. **Cerebral blood volume maps of gliomas: comparison with tumor grade and histologic findings.** *Radiology* 1994;191:41–51
8. Nussbaum E, Djalilian H, Cho K, et al. **Brain metastases: histology, multiplicity, surgery, and survival.** *Cancer* 1996;78:1781–88
9. Lu W, Bucana CD, Schroit AJ. **Pathogenesis and vascular integrity of breast cancer brain metastasis.** *Int J Cancer* 2007;120:1023–26
10. Onodera H, Nagayama S, Tachibana T, et al. **Brain metastasis from colorectal cancer.** *Int J Colorectal Dis* 2005;20:57–61
11. McCurley CR, Shivers RR, Del Maestro RF. **Quantitative comparison of the morphology of the microvasculature of primary lung lesions and metastatic brain tumors.** *J Submicrosc Cytol Pathol* 1998;30:257–69
12. Sangiorgi S, Congiu T, Manelli A, et al. **The three-dimensional microvascular architecture of the human Kaposi sarcoma implanted in nude mice: A SEM corrosion casting study.** *Microvasc Res* 2006;72:128–35. Epub 2006 Aug 22
13. Donahue KM, Krouwer HGJ, Rand SD, et al. **Utility of simultaneously acquired gradient-echo and spin-echo cerebral blood volume and morphology maps in brain tumor patients.** *Magn Reson Med* 2000;43:845–53
14. Sugahara T, Korogi Y, Kochi M, et al. **Perfusion-sensitive MR imaging of gliomas: comparison between gradient-echo and spin-echo echo-planar imaging techniques.** *AJNR Am J Neuroradiol* 2001;22:1306–15
15. Speck O, Chang L, DeSilva NM, et al. **Perfusion MRI of the human brain with dynamic susceptibility contrast: gradient-echo versus spin-echo techniques.** *J Magn Reson Imaging* 2000;12:381–87
16. Calli C, Kitis O, Yunten N, et al. **Perfusion and diffusion MR imaging in enhancing malignant cerebral tumors.** *Eur J Radiol* 2006;58:394–403
17. Cha S, Tihan T, Crawford F, et al. **Differentiation of low-grade oligodendrogliomas from low-grade astrocytomas by using quantitative blood-volume measurements derived from dynamic susceptibility contrast-enhanced MR imaging.** *AJNR Am J Neuroradiol* 2005;26:266–73
18. Boxerman JL, Schmainda KM, Weiskoff RM. **Relative cerebral blood volume maps corrected for contrast agent extravasation significantly correlate with glioma tumor grade, whereas uncorrected maps do not.** *AJNR Am J Neuroradiol* 2006;27:859–67